

A MINIATURE COLD ATOM FREQUENCY STANDARD

V. Shah¹, M. Mescher², A. Martins¹, J. Leblanc², N. Byrne²,
B. Timmons², R. Stoner², F. Rogamentich², and R. Lutwak¹

¹Symmetricom, Technology Development Center, Beverly, MA 01915

²The Charles Stark Draper Laboratory, Cambridge MA, 02139

E mail: *vshah@symmetricom.com*

Abstract

We report on our progress towards the development of a miniature cold atom frequency standard (MCAFS). The ultimate program objective is a chip-scale atomic clock (CSAC) with performance comparable to a bench top Cesium beam primary standard. Utilizing microwave interrogation of a freely-expanding cloud of laser-cooled atoms, the MCAFS eliminates the two primary sources of uncertainty in existing CSACs, namely buffer gas collisions and the AC Stark (light) shift. Compared to conventional cold atom frequency standards, such as atomic fountain clocks, achieving the required 1000-fold reduction of size and power necessitates considerable simplification of the clock architecture and the development of novel components, fabrication techniques, and operational algorithms.

SECTION I. INTRODUCTION

Recent advances in the technology and miniaturization of vapor cell atomic frequency standards have produced chip-scale atomic clocks (CSACs), with suitably low size, weight, and power (SWAP) for integration in handheld battery-operated devices [1,2]. This new generation of atomic clocks enables new applications and architectures for secure communications and navigation, remote sensing and data logging, as well as future applications in ad hoc networking, high-bandwidth portable communications, inertial guidance, and calibration. While vapor cell clocks excel at providing precise timing over short time scales, they are inherently susceptible to frequency errors due to thermal and other environmental perturbations as well as long-term aging over longer time scales ranging from several days to weeks. Vapor cell clocks also suffer from a lack of absolute accuracy which necessitates periodic recalibration for the vast majority of applications. The two largest contributions to inaccuracies and drifts in vapor cell clocks arise from (i) buffer gas induced pressure shifts [3], and (ii) light-shifts [4]. While it is possible to minimize or eliminate the light-shifts, buffer gas pressure shifts cannot be completely eliminated without eliminating the buffer gas itself. Further performance improvement in compact, low-power frequency standards requires a fundamentally different technology.

Atomic frequency standards based on thermal atomic beam technology [5], developed in the 1950's, are far more accurate than gas cell clocks because they eliminate buffer gas and do not rely on optical detection, which perturbs the frequency due to the AC Stark Shift ("the light shift"). Atomic beam clocks are significantly larger, more expensive, and power hungry compared to vapor cell clocks, but even today they play a critical role in applications where absolute frequency accuracy is essential. Unfortunately, miniaturizing atomic beam technology would severely compromise its performance. In large part this is because the short term instability is proportional to the interrogation time, which is determined by the velocity (temperature) of the beam and the size of the package.

Atomic "fountain" clocks [6], based on laser cooled atoms, developed in the 1990s, have largely replaced thermal beam clocks for the highest accuracy application, such as primary national time standards.

Fountain clocks have excellent short-term stability (STS) and accuracy but have yet to see application outside of laboratory environments, due to size, complexity, and environmental sensitivity. Compared to thermal beam technology, the dimensional scaling laws for fountain clock technology are considerably more favorable, making them more attractive for evolution to ultimately achieve CSAC-like SWAP.

In this paper, we report on our progress towards development of a chip-scale atomic clock based on a freely-expanding cloud of laser-cooled cesium atoms. The Miniature Cold-Atom Frequency Standard (MCAFS) is based on the same principles as a fountain clock and therefore is expected to provide excellent frequency accuracy and low drift. The primary functional difference between the MCAFS and an atomic fountain clock is the duration of the interval over which the atomic frequency is interrogated. In the fountain clock, atoms are tossed upwards by approximately a meter, in order to provide longest possible time for frequency measurement, in MCAFS the cold atoms are allowed to drip from the trap and the frequency measurement is carried out before atoms fall, due to gravity, by no more than 2 mm.

The MCAFS has been designed for robust deployment in portable instruments. A great deal of emphasis has been placed on reducing its complexity, volume and power consumption as well as to improve mechanical robustness, and insensitivity to shock, vibration, and orientation. Some of the steps that we took to simplify the design of MCAFS are summarized below. Many of these steps are based on previous advances in the field and by a number of researchers over the last two decades.

- **Single Diode Laser:** Traditionally, multiple frequency-stabilized laser sources have been used for laser cooling and trapping [7], optical pumping [8] and resonant detection. Instead, the MCAFS uses a single diode laser to sequentially perform multiple roles at different times during the clock cycle.
- **Laser Frequency Stabilization:** We have developed a miniature, very low power dichroic atomic vapor laser lock assembly (DAVLL) [9]. The DAVLL enables a high-bandwidth servo to stabilize the laser frequency and to rapidly and accurately adjust the laser frequency over a wide range. To maintain high absolute laser frequency accuracy, the DAVLL is periodically calibrated during operation based on the cold atom fluorescence signal, without interrupting the normal clock operation.
- **Pyramidal MOT:** The conventional magneto-optical trap (MOT) requires six independent circularly-polarized laser beams. The MCAFS uses a single beam combined with a conical mirror to conserve volume and reduce tight constraints on beam alignment [10].
- **Microwave Interrogation:** In the fountain clock geometry, the atoms pass through a microwave cavity twice during its upward and downward trajectory. In MCAFS, the atomic frequency measurement is carried out in just 15 ms (compared to over 1 s in traditional fountain clock), during which time the atoms are displaced by less than 2 mm.

SECTION II. MCAFS CONSTRUCTION

Figure 1 shows a picture of the MCAFS prototype. On the left-most side of the MCAFS is a temperature stabilized laser diode. The light emitted by the laser is collimated and the astigmatic divergence is corrected by a pair of cylindrical lenses. A thin glass plate directs a weak sample of the beam (4%) towards the DAVLL for stabilizing and controlling the laser frequency. The main part of the laser beam passes through an optical shutter with a high extinction ratio. The beam is then expanded by a two-lens telescope, circularly polarized, and directed onto the MOT cell assembly. Within the MOT cell, the atoms are slowed down to a few tens of centimeters per second by resonant scattering from the laser beam and trapped localized in the center of the cell by magnetic field gradients created by a pair of coils outside of the cell. The fluorescence signal from the atoms is detected by an annulus of photodiodes placed outside of the MOT cell at a distance of about 1 cm. A small loop of wire outside of the glass window is used to

apply microwave pulses for excitation of the microwave resonance. The key components of the MCAFS are described in greater detail below.

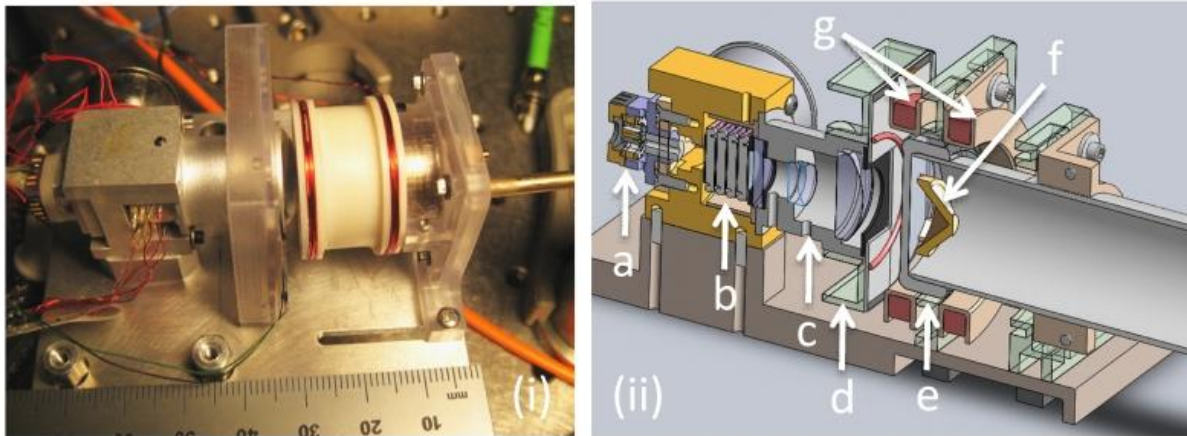


Figure 1. (i) Photograph of the Miniature Cold-Atom Frequency Standard (MCAFS) (ii) 3D cross-sectional view (a) packaged diode laser, (b) optical shutter, (c) expansion lenses and quarter wave plate, (d) photodiode array, (e) UHV chamber, (f) copper cone, and (g) magnetic field coils.

LASER SOURCE

All optical frequencies necessary for MCAFS are provided by a single 852 nm distributed Bragg reflector (DBR) semiconductor laser. The DBR laser is a custom device, manufactured by Photodigm, Inc., which employs a dual quantum well architecture for high-efficiency modulation at GHz frequencies and is designed to tune to the cesium D2 wavelength at 852.354 nm at a relatively high temperature ($>40^{\circ}\text{C}$). The spectral line-width of the laser is < 3 MHz measured in a 200 Hz bandwidth. The laser was mounted on a thermoelectric cooler (TEC) inside a ceramic package (see Figure 2). The TEC stabilized the laser temperature and was used for coarse tuning of the laser wavelength.

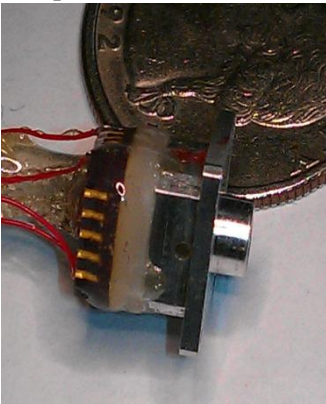


Figure 2. A packaged DBR laser leadless-chip-carrier with a thermoelectric cooler and a cylindrical lens.

The laser is principally operated on the $6S_{1/2}, F=4 \rightarrow 6P_{3/2}, F=5$ “cycling” transition for laser cooling and state detection. In order to generate a small amount of power ($\approx 1\%$) at a second laser wavelength, detuned by 8.92 GHz to the $6S_{1/2}, F=3 \rightarrow 6P_{3/2}, F=3$ “repumping” transition, microwave modulation is applied to the bias current of the laser. The double quantum well DBR laser displays >3 GHz modulation bandwidth, which is considerably higher than most edge-emitting diode lasers but, unfortunately, was still not sufficient to provide efficient sideband generation at 8.92 GHz. For this reason, the laser is modulated at one-half of the desired sideband detuning, 4.46 GHz, and the second-order sideband is used for repumping. The second order sideband contains roughly 1% of the total laser power.

DAVLL ASSEMBLY

As shown in the photograph of Figure 3(a) and the cross-section of Figure 3(b), the DAVLL assembly is nearly identical to the 1 cm³ Chip-Scale Atomic Clock physics package developed by Symmetricom and Draper Laboratory under Phase-II of the DARPA CSAC program [11], except that the internal laser has been removed and a window has been added to the bottom of the package to permit application of the external laser beam. The key components of the DAVLL assembly are (1) a thermistor, (2) cesium vapor cell, and (3) photodiode. A permanent magnet (4) is glued on the back side of the DAVLL assembly to provide roughly 50 Gauss magnetic field. The assembly is enclosed in a custom single layer magnetic shield, to reduce the fringing fields from the magnet from interfering with the clock frequency measurement.

The optical geometry of the DAVLL assembly, shown in Figure 3(c), is similar to that of a traditional DAVLL, with the exception that for simplicity we use a single photodiode for polarimetry instead of conventional balanced polarimetry using two photodiodes. This affords a simple linear geometry which is straightforward to implement in a compact, robust package.

The first iteration DAVLL is hermetic, but not vacuum sealed. Nonetheless, the total power consumption of the DAVLL assembly is less than 30 mW, almost all of which was utilized to heat the cesium vapor cell (containing no buffer gas) to 55°C. In subsequent iterations, with the addition of vacuum packaging, the power consumption will be reduced to less than 10 mW.

OPTICAL SHUTTER

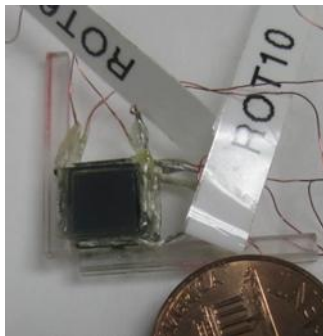


Figure 4. LCD shutter.

A custom optical switch is used to rapidly turn-on and -off the laser light falling on the MOT cell. The optical switch is constructed by precisely aligning a stack of liquid crystal display (LCD) polarization rotators with a high extinction ratio polarizer placed between each rotator. The extinction ratio of the combined LCD optical switch is greater than 60 dB, with a rise/fall time less than 0.1 ms. The insertion loss of the switch is less than 3 dB. A picture of the LCD switch is shown in Figure 4. The LCD switch consumed negligible power and its total volume is roughly 1 cm³.

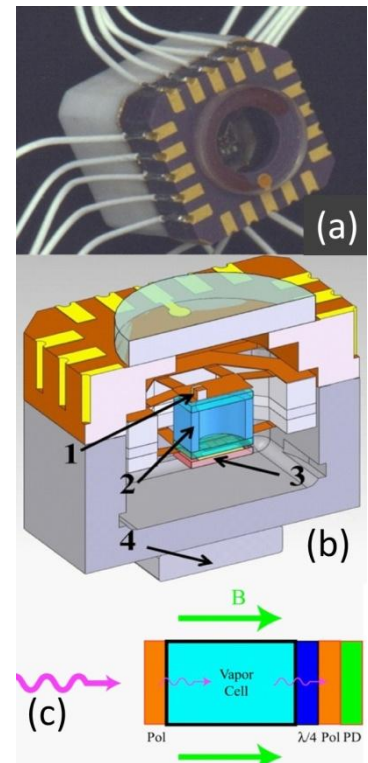


Figure 3. MCAFS DAVLL assembly (a) Photo (b) cross-section and (c) geometry.

MOT CELL

The cold atoms are collected and interrogated within the MOT cell, which is a high-vacuum enclosure containing the conical mirror behind a large aperture window for illumination and detection of the atomic sample.

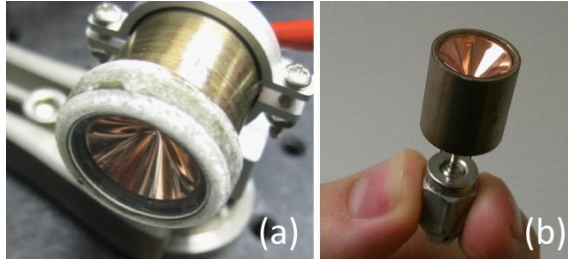


Figure 5. MOT Cell (a) Phase-I (b) Phase-II.

While the early prototypes have used a tabulated cell, connected to a small vacuum-ion pump, we would ultimately like to develop a completely sealed system, pumped only by non-evaporable getter (NEG) material sealed within the cell. We thus require that the cell be compatible with a high-temperature bakeout process to eliminate contaminants. Also, the window must be comprised of a transparent material which is not permeable to helium, which is not pumped effectively by NEG. Figure 5(a) shows the MOT cell which was used to obtain the results of this paper. It is constructed from non-magnetic stainless steel with a Corning 1720 helium-impermeable glass window at the front. A 1/8th inch tube attached to the back side of the cell is used to maintain ultra-high vacuum in the cell using a miniature 2 l/s ion pump. The dimensions of this “Phase-I” MOT cell are 0.7 cm (OD) x 1.8 cm (L) and the outside volume is 5.2 cm³.

Figure 5(b) shows our next-generation “Phase-II” MOT cell, with a titanium body, sapphire windows, and a 1/16th inch OD pump-out tube. The sapphire windows are brazed directly to the titanium body which reduces distortion at the edges of the window. These new cells are roughly half the size of the Phase-I device, 1.4 cm (OD) x 1.8 cm (L).

Inside the MOT cell, a 1.6 cm diameter, highly reflective copper cone faces the glass window. The copper cone is fabricated by an electroforming 0.38 mm of OFHC copper onto a diamond-turned aluminum mandrel as shown in Figure 6. The conical surface of the mandrel is polished to a surface roughness of less than 80 nm rms. For future versions of MCAFS, as we continue to reduce the size, the copper cones may be sawn to a smaller diameter.

The MOT cell also contains an alkali metal dispenser (AMD) and a non-evaporable getter (NEG). The AMD maintains constant cesium background pressure in the chamber and the role of the NEG is to improve the vacuum in the chamber. To provide the necessary magnetic field for trapping cold atoms, a pair of magnetic coils, driven in the anti-Helmholtz configuration, are mounted outside the cell, thereby creating a magnetic field with a magnetic field minimum near the center of the cone.

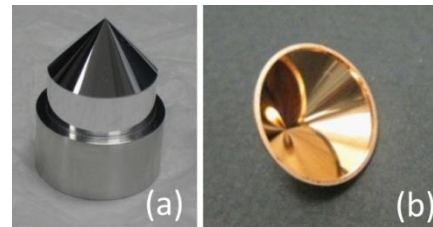


Figure 6. (a) Diamond turned aluminum mandrel, (b) Electroformed copper cone.

SIGNAL RECOVERY

The fluorescence signal from the trapped atoms is monitored by an annular ring of photodiodes, as shown in Figure 1(ii)(d). The photodiode ring is carefully positioned to be outside the direct line-of-sight of the laser light reflected by the cone. Nevertheless, a significant 2-3% of the background light is scattered by the glass window and the copper cone and these stray reflections dominate the detected signal. In relative units, the typical contribution to the photodiode signal from various sources is as follows: (i) 70% scattered light from the copper cone and the front window, (ii) 10-40% scattered light by the thermal cesium vapor, depending on the cesium vapor pressure, (iii) 20% resonance-fluorescence from atoms trapped in a MOT.

The actual clock signal consists of only the fraction of the cold atoms which are initially in the $|F=3, m_f=0\rangle$ and which are transferred to the $|F=4, m_f=0\rangle$ state, roughly $1/10^{\text{th}}$ of the cold-atom signal, i.e. $\approx 2\%$ of the total detected signal. With this signal level, the signal/noise ratio is dominated by the noise which arises from laser frequency noise, converted to amplitude noise by resonant scattering from both the cold cesium atoms and the background (thermal) atoms in the MOT cell (FM-AM conversion). In smaller MOT cells, however, the relative-intensity-noise (RIN) from the scattered light begins to dominate because there are fewer cold atoms contributing to the FM-AM conversion.

SECTION III. MCAFS OPERATION

To achieve ultra-high vacuum in the MOT cell, it is degassed by baking under high vacuum at 350°C for 48 hours. After baking, the MOT cell is cooled down to room temperature and cesium is introduced into the cell by passing several amperes of current through the AMD. Initial conditioning of the cell requires several hours of AMD operation, during which excess cesium is released in the chamber, which is “gettered” by the cell walls and other reactive surfaces until they are saturated with cesium. Following this first activation, the cesium vapor pressure settles into quasi-equilibrium within 24 to 48 hours.

Subsequently, the cesium vapor pressure decays slowly with a time constant ranging from several days to weeks depending on the length of the initial activation. Additional short activations are periodically required to maintain the optimum quasi-equilibrium vapor pressure for laser cooling. For efficient MCAFS operation, the optimum background cesium vapor pressure is such that the loading rate of the cold atoms in the MOT is a few seconds. When reactivation is necessary, the AMD is operated for several minutes in “pulsed” mode, interleaving the high-current drive synchronously with the laser cooling part of the clock cycle so that the magnetic perturbation due to the high current drive was not present during the frequency measurement part of the cycle and thereby avoiding intermittent perturbations to the clock output frequency.

The expansion telescope generates a collimated laser beam, approximately 1.5 cm in diameter, which uniformly illuminates the input aperture of the MOT cone, through the MOT cell window. The laser light is circularly polarized and slightly red-detuned from the $F=4$ to $F'=5$ transition. As a result of multiple reflections from the polished conical surface, the atoms at the center are exposed to circularly-polarized light incident from all directions, the scattering of which slows them down to extremely low velocities and collects them at the magnetic field minimum at the center of the MOT. The number of atoms captured in a MOT has a very strong dependence on the diameter of the cone. For a medium-sized cone (0.5 to 2 cm), the number of atoms captured in a MOT scales as the fourth power of the cone diameter. The atom number dependence has been shown to be even stronger (sixth power) for cone diameters that are even smaller [12]. Figure 7 shows the typical atom number we observed in our MOT as a function of cone diameter for constant intensity. The atom number in our system agrees well with the theoretical d^4 relation.

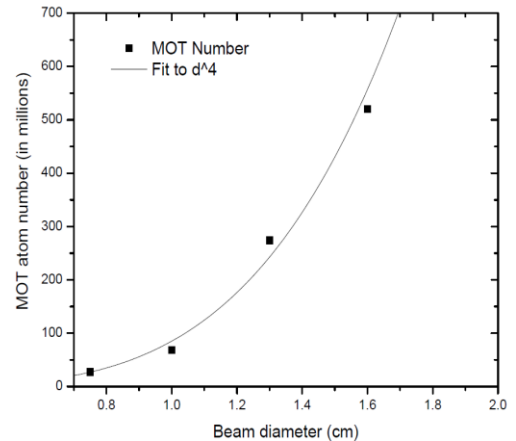


Figure 7. Scaling of MOT collection efficiency with size.

The MCAFS can be operated in either of two modes, utilizing either a single “Rabi” pulse, with microwave power and time adjusted to provide complete “ π ” inversion of the sample or using the Ramsey separated oscillatory fields method, in which the interrogation is split between two “ $\pi/2$ ” pulses. The Ramsey method produces a slightly narrower resonance signal but adds the complexity of identifying which of the interference fringes is the central clock transition.

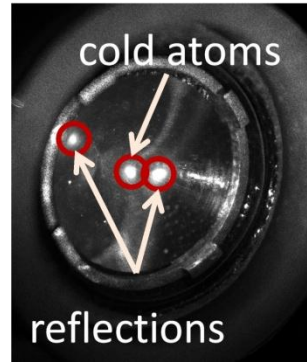


Figure 8. Cold Atoms in MCAFS.

The following is a typical MCAFS clock cycle, utilizing the Ramsey method. In this example, the total duration of the interrogation cycle is 205 ms. At $t=0$, the optical shutter, the laser microwave modulation, the MOT coils are all turned on. The laser is initially tuned roughly 10 to 15 MHz red of the $F=4$ to $F'=5$ cesium transition. Atoms are collected in the MOT for 180 ms. At $t = 180$ ms, the magnetic field is switched off and the laser is detuned further red for further “molasses” cooling. At $t = 183$ ms, the microwave modulation repump sideband is turned-off and the laser is tuned onto the $F=4$ to $F'=5$ resonance, which causes all of the atoms to be optically pumped into the $F=3$ ground state. At $t = 187$ ms, the optical shutter is closed, leaving the atoms freely suspended in the dark. At the same time, the laser is moved far-off resonance (roughly 125 MHz red of the $F=4$ to $F'=5$ transition) so that any leakage light produces minimal shift of the clock resonance measurement. At $t = 188$ ms, a 1 ms long, $\pi/2$ microwave interrogation pulse is applied using the microwave loop, at the frequency of the $|F=3, m_f=0\rangle$ and $|F=4, m_f=0\rangle$ magnetically insensitive ground state hyperfine frequency. A second $\pi/2$ pulse is applied 15 ms later, at $t = 203$ ms. Between the two $\pi/2$ microwave pulses, the atomic superposition state evolves freely, in the dark, as the cloud of atoms expands slightly due to thermal motion and falls ≈ 1 mm under the influence of gravity. The displacement of the atoms under gravity and due to thermal expansion creates perhaps the largest systematic shift in the clock, which we estimate to be on the order of 1 part in 10^{11} . We are currently exploring ways to minimize this shift.

At $t = 204$ ms, the laser is tuned to the $F=4$ to $F'=5$ optical resonance and the optical switch is opened. The initial fluorescence signal from the cold atoms in 1 ms indicates the number of atoms transferred to $|F=4, m_f=0\rangle$ ground state by the microwave pulse. Since the number of atoms that are transferred to the $|F=4, m_f=0\rangle$ ground state is a function of the detuning of the applied microwave frequency from cesium hyperfine resonance frequency, the information about the number of atoms in the $|F=4, m_f=0\rangle$ state is used to lock the microwave frequency to the cesium ground state hyperfine frequency.

At 205 ms, a new clock cycle begins starting with re-trapping cold atoms from the previous cycle. We typically achieve re-cycling efficiencies close to 60%, limited mostly by the background vapor pressure and the absolute temperature of the cold atom.

SECTION IV. EXPERIMENTAL RESULTS

The experimental results presented below were carried out with an MCAFS that was identical to the one shown in Figure 1, with the exception that a small optical isolator, 1.5 cm (d) x 1.5 cm (h), was additionally included in the physics package, placed directly in front of the laser. The optical isolator improves the clock stability and allows uninterrupted clock operation for extended time periods. Unfortunately, millimeter scale optical isolators with relatively low insertion loss are not available at the cesium D2 wavelength (852 nm). The next generation of MCAFS will employ rubidium, rather than cesium, for which millimeter scale optical isolators are available off-the-shelf at the required (780 nm) wavelength. Figures 9(a) and 9(b) show Ramsey and Rabi microwave resonances, respectively, observed by sweeping the frequency of the microwave local oscillator. The linewidth of the Rabi resonance is 50 Hz (full-width), limited by the Fourier transform of the 15 ms interrogation time. The center of the microwave resonance is frequency shifted by ≈ 105 Hz by the ambient earth's magnetic field.

To operate the MCAFS as a clock, the standard technique of synchronous modulation of the LO and demodulation of the recovered population inversion signal (number of atoms in the $|F=4, m_f=0\rangle$ state) is used to generate an error signal proportional to the relative detuning, and the LO is thereby servoed to the peak of the atomic microwave resonance.

Figure 10 shows the instability (Allan deviation) of the LO frequency when operated with the servo enabled. The Allan deviation shows the $\tau^{-1/2}$ behavior which is characteristic of passively-interrogated atomic clocks. Over time scales longer than 10,000 seconds, the clock frequency shows some drift, which we attribute due to the lack of magnetic field shielding on this prototype device. The 2×10^{-11} / $\sqrt{\text{Hz}}$ STS in MCAFS is principally limited by frequency noise on the laser.

SECTION V: CONCLUSION

We have developed a fully integrated low-power cold atom system that fits on a palm top. The prototype relies on a single laser locked to an agile miniature DAVLL to sequentially perform the role of multiple lasers traditionally used cold atom systems. For laser cooling, we use a conical mirror MOT to significantly simplify the optical setup. The volume of the MCAFS physics package is 75 cm³, including the complete laser system, optical shutter, DAVLL assembly, beam expansion optics and the UHV

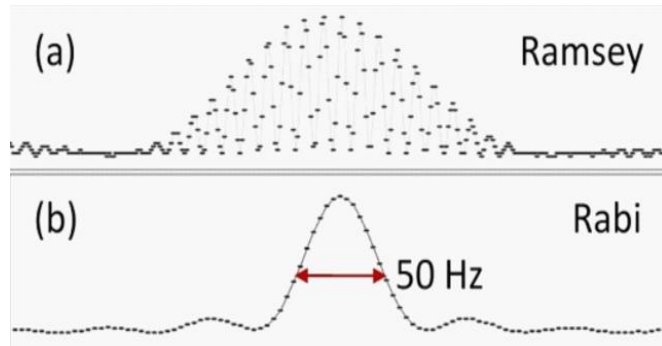


Figure 9. MCAFS Microwave resonance utilizing (a) Ramsey and (b) Rabi interrogation

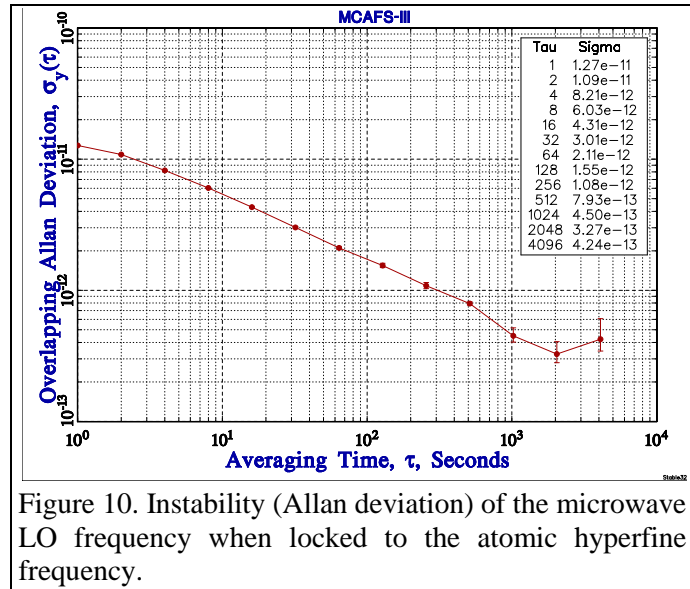


Figure 10. Instability (Allan deviation) of the microwave LO frequency when locked to the atomic hyperfine frequency.

chamber. When run as clock, MCAFS yields short term instability of 2×10^{-11} / $\sqrt{\text{Hz}}$. MCAFS can be adapted for use in other applications such as magnetometry and atom interferometers [13].

ACKNOWLEDGEMENTS

The authors would also like to thank Prof. Vladan Vuletic, Andrew Grier and Monica Schleier-Smith of MIT, and Don Emmons and Mike Garvey of Symmetricom. This project was funded by the Defense Advanced Research Projects Agency (DARPA), Contract # N66001-09-C-2057.

DISTRIBUTION STATEMENT

Distribution Statement "A" (Approved for Public Release, Distribution Unlimited).

DISCLAIMER

The views expressed are those of the author and do not reflect the official policy or position of the Department of Defense or the U.S. Government.

REFERENCES

- [1] S. Knappe, *et al.*, 2004, "A microfabricated atomic clock," **Applied Physics Letters**, Vol. 85, no. 9, 1460.
- [2] R. Lutwak, P. Vlitias, M. Varghese, M. Mescher, D. K. Serkland, and G. M. Peake, 2005, "The MAC – a miniature atomic clock," in Frequency Control Symposium and Exposition, Proceedings of the 2005 IEEE.
- [3] M. Arditi and T. R. Carver, 1961, "Pressure, Light, and Temperature Shifts in Optical Detection of 0-0 Hyperfine Resonance of Alkali Metals," **Physical Review**, Vol. 124, no. 3, 800-809, Nov. 1961.
- [4] W. Happer and B. S. Mathur, 1967, "Effective Operator Formalism in Optical Pumping," **Physical Review**, Vol. 163, no. 1, 12, Nov. 1967.
- [5] R. E. Beehler, R. C. Mockler, and J. M. Richardson, 1965, "Cesium Beam Atomic Time and Frequency Standards," **Metrologia**, Vol. 1, 114-131, Jul. 1965.
- [6] R. Wynands and S. Weyers, 2005, "Atomic fountain clocks," **Metrologia**, Vol. 42, S64-S79, Jun. 2005.
- [7] C. Monroe, W. Swann, H. Robinson, and C. Wieman, 1990, "Very cold trapped atoms in a vapor cell," **Physical Review Letters**, Vol. 65, no. 13, 1571.
- [8] W. Happer, 1972, "Optical Pumping," **Reviews of Modern Physics**, Vol. 44, no.2, 169, Apr. 1972.

- [9] K. L. Corwin, Z.-T. Lu, C. F. Hand, R. J. Epstein, and C. E. Wieman, 1998, “*Frequency-Stabilized Diode Laser with the Zeeman Shift in an Atomic Vapor*,” **Applied Optics**, Vol. 37, no. 15, 3295-3298, May 1998.
- [10] K. I. Lee, J. A. Kim, H. R. Noh, and W. Jhe, 1996, “*Single-beam atom trap in a pyramidal and conical hollow mirror*,” **Optics Letters**, Vol. 21, no. 15, 1177-1179.
- [11] M. J. Mescher, R. Lutwak, and M. Varghese, 2005, “*An ultra-low-power physics package for a chip-scale atomic clock*,” in The 13th International Conference on Solid-State Sensors, Actuators and Microsystems, 2005, Digest of Technical Papers: Transducers – ’05, Vol. 1, pp. 311-316.
- [12] S. Pollock, J. P. Cotter, A. Laliotis, F. Ramirez-Martinez, and E. A. Hinds, 2011, “*Characteristics of integrated magneto-optical traps for atom chips*,” **New Journal of Physics**, Vol. 13, p. 043029, Apr. 2011.
- [13] Q. Bodart, S. Merlet, N. Malossi, F. P. Dos Santos, P. Bouyer, and A. Landragin, 2010, “*A cold atom pyramidal gravimeter with a single laser beam*,” **Applied Physics Letters**, Vol. 96, p. 134101.